



Conference Paper

Welding lines prediction in numerical analysis of porthole die extrusion processes and welding quality estimation through a novel experimental approach

Author(s):

Crosio, Michele; Hora, David; Hora, Pavel

Publication Date:

2019

Permanent Link:

<https://doi.org/10.3929/ethz-b-000386358> →

Rights / License:

[In Copyright - Non-Commercial Use Permitted](#) →

This page was generated automatically upon download from the [ETH Zurich Research Collection](#). For more information please consult the [Terms of use](#).

WELDING LINES PREDICTION IN NUMERICAL ANALYSIS OF PORTHOLE DIE EXTRUSION PROCESSES AND WELDING QUALITY ESTIMATION THROUGH A NOVEL EXPERIMENTAL APPROACH

Michele Crosio¹, David Hora² and Pavel Hora¹

¹ETH Zurich, Institute of Virtual Manufacturing, Tannenstrasse 3, 8092 Zurich, Switzerland, michele.crosio@ivp.mavt.ethz.ch, pavel.hora@ivp.mavt.ethz.ch

²inspire AG – IVP (Institute of Virtual Manufacturing), Technoparkstrasse 1, 8005 Zurich, Switzerland, david.hora@inspire.ethz.ch

Keywords: Aluminium extrusion, Seam welds, Finite element method, Particle-tracking, Solid-state welding

Abstract. A result of the extrusion of hollow profiles, by means of porthole dies, is the presence of seam welds along the entire length of the extrudate. In order to avoid lower quality profiles due to reduced mechanical properties of the welds, it is crucial to ensure an adequate welding quality throughout the entire length of the product. The aim of this study is to propose two experimental approaches to calibrate welding criteria for their further implementation in FE-simulations of extrusion processes. By means of FE-simulations, different experimental conditions have been analyzed and different welding criteria compared. Moreover, a numerical methodology is presented, integrated within the special purpose FE-software PF-Extrude, for the evaluation of the considered quality criteria during the analysis of seam welds within extrusion processes.

Introduction

The extrusion process allows great flexibility within the geometries of profiles that can be therewith manufactured. During the extrusion of hollow profiles, a common technique is the use of porthole dies: by means of legs, the billet is pressed and divided into different material streams through the portholes. As the material flows into the welding chamber, the streams are rejoined. Ultimately, the material reaches the outlet of the die, where the outer geometry is defined by the cap of the die, while the inner contour of the profile is shaped by a mandrel (Fig. 6 a). It is critical for the quality of the extrudate that the different material streams bond together and, being the extrusion process a non-stationary process, this must be ensured over the entire length of the product. It is an industrial praxis to analyze the quality of the seam welds by means of destructive methods, where the extruded profile is sectioned at different regions and analyzed under different loading conditions.

In order to prevent extensive time-consuming and costly analysis, FE-methods allow virtual analysis of the seam welds, giving insights over the product before the die is manufactured. Efforts have been made to develop criteria, which describe the solid-state welding quality during the process: within the literature, it is possible to find the Q criterion by Plata and Piwnik [1]. The criterion describes the welding quality as the time integration of the triaxiality value η (defined as hydrostatic pressure p over effective stress σ_v) following a material point along the welding zone (Eq. 1).

$$Q = \int \eta \cdot dt = \int \frac{p}{\sigma_v} \cdot dt. \quad (1)$$

In the research conducted by Donati and Tomesani [2] it has been shown that the material can have very high residence times close to the dead metal zones, causing the integration of the Q criterion to assume high values for material being exhausted by these regions. For this reason, the K-criterion has been proposed, which is formulated as the path integral (given the velocity vector and the time increment) of the stress triaxiality (Eq. 2).

$$K = \int \eta \cdot v \cdot dt = \int \frac{P}{\sigma_v} \cdot dl . \quad (2)$$

Moreover, the criterion has been tested with experimental and FEM analysis campaigns through the Valberg experiment, whereby an H-shaped profile is extruded with a seam weld in the middle [3, 4]. The results showed a good accordance of the K-criterion with the experiments.

J. Yu et al. [5] explored the influence of temperature during the solid state welding of seam welds: the developed J-criterion is described as the time integral of stress triaxiality and strain rate, scaled with an exponential function of the temperature (Eq. 3).

$$J = \int k_0 \cdot \eta \cdot \dot{\varepsilon} \cdot \exp\left(\frac{RT}{Q_D}\right) \cdot dt \quad (3)$$

whereby k_0 represents a surface quality scaling factor (in the research assumed to be $k_0 = 1$), $R = 8.314 \text{ J mol}^{-1} \text{ K}^{-1}$ is the universal gas constant and Q_D describes the diffusion activation energy. In the study, a literature value $Q_D = 1.42 \times 10^5 \text{ J mol}^{-1}$ (within the temperature range 450-650°C) for aluminium has been used.

The temperature effect during solid state welding has been analyzed by E. Ceretti et al. [6], whereby the welding condition of AA6061 specimens has been investigated by means of flat rolling experiments at different rolling ratios and temperatures. Thereby, the criterion by Plata and Piwnik has been implemented in the FEM simulations and evaluated for each experiment. The results showed a clear dependency of the welding phenomenon to the temperature, showing different Q-values at each different temperature. In particular, the results showed lower Q-values, required to achieve bonding, at higher temperatures.

In order to analyze the bonding condition of alloy AA6082, S. W. Bai et al. [7] developed an experimental set-up, where two aluminium cylindrical bars are compressed together inside a closed welding chamber. As the compression progresses and the chamber is filled, the material from the two specimens weld together. The set-up has been designed such that the bonding condition between the probes can be tested under different loads and at various temperatures. Furthermore, the welded probes have been investigated through tensile tests. The experimental set-up was able to recreate the hydrostatical pressure, which forms during the extrusion process, and different welding conditions could have been reproduced by varying the experimental process parameters (punch velocity, stroke and temperature).

It is the intention of this study to propose two laboratory experimental set-ups in order to calibrate the considered welding criteria. By means of FE-simulations, these have been compared, showing the problematic of solid-state welding criteria and their implementation in extrusion virtual analysis. Moreover, a seam-welds-quality evaluation routine integrated within the special ALE (Arbitrary Lagrangian Eulerian) FE-code [8] PF-Extrude is presented.

FE modeling of experimental approaches

Two different experimental set-ups are proposed in order to calibrate the quality criteria for the evaluation of the bonding condition of seam welds for arbitrary profiles.

Tools of experiments. The first experimental set-up proposed (Fig. 1 a) consist in the compression of two specimens inside a container. Thereby, the specimens (Fig. 1 b) are manufactured with a conical tip, such that the material can deform within the container as the pressure increases. The set-up is provided with heating cartridges, in order to execute the experiments at different temperatures. The bonded specimens can be analyzed under tensile conditions and by means of microstructure analysis.

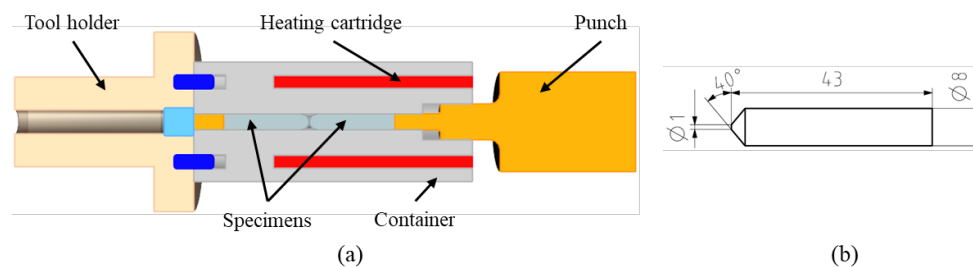


Fig. 1. (a) Tools of first experimental set-up, (b) design of specimen.

The second experimental set-up (Fig. 2 a) is based on the backward cup extrusion process, whereby the extruded material flows in the opposite direction of the punch movement. The specimen to be extruded is composed by two different parts that fit together (Fig. 2 b): the first is a cylindrical probe where a conical pocket has been machined. The second conical probe is inserted in the pocket, completing the specimen. The diameter of the punch defines the extrusion ratio, which can be varied in order to reach different states of the hydrostatic pressure. By controlling the stroke of the punch, the contact time and the strain of the material can be varied. Moreover, the set-up can be tested at different temperatures. The bonding condition can be analyzed through an analysis of the microstructure at the contact interface between the two probes.

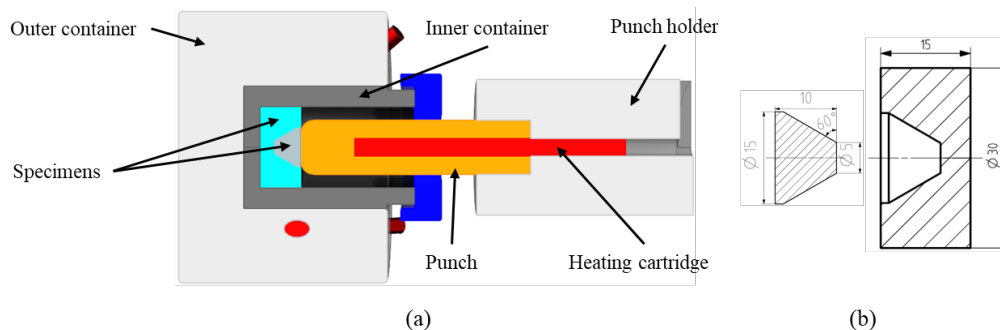


Fig. 2. (a) Tools of second experimental set-up, (b) designs of specimens.

FE - analysis. The tooling set-ups have been simulated with simufact.forming by means of 2D axis-symmetrical analysis. The first set-up has been further simplified, assuming that the deformation of the two probes is specular. Therefore, the specimen is compressed in the simulation against a static stopper tool (Fig. 3 a). All the simulations have been carried out with the shear-friction model, whereby a coefficient $m = 0.6$ has been chosen for the contact

between the specimen and -both- the container and the pusher. On the other hand, a friction coefficient $m = 0.9$ has been chosen for the contact condition between specimen and stopper (simulating the contact with the second specimen) for the first set-up and between the two specimens for the second set-up (Fig. 3 b, c).

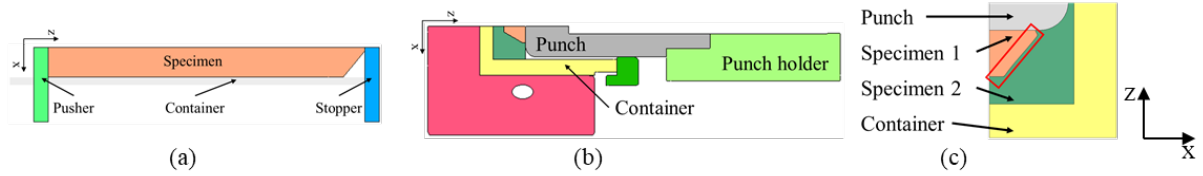


Fig. 3. (a) FE-model of the first experimental set-up, (b) FE-model of the second experimental set-up (c) evaluation region of the second experiment (marked red)

A subroutine has been programmed in order to evaluate the Q, K and J criterion at the contact interface between the specimens (in the first set-up this is represented by the contact with the stopper). The routine is called at the end of every simulation increment and a contact check is executed: if a node of the first specimen is in contact with the second, the three criteria are integrated over the time step of the simulation and the Q-, K- and J- values updated.

Material modeling. The yield behavior of the considered aluminium alloy AA6060 has been retrieved through dilatometer tests, whereby probes have been tested at different temperatures and compression rates. The experimental data has been fitted with the Hensel-Spittel model (Eq. 4) in order to be used during the simulations in simufact. The fitted parameters can be found in table 1.

$$k_f(T, \dot{\varepsilon}, \varepsilon) = A \cdot \exp(m_1 \cdot T) \cdot \varepsilon^{m_2} \cdot \exp\left(\frac{m_4}{\varepsilon}\right) \cdot \dot{\varepsilon}^{m_3} \quad (4)$$

Table 1. Fitting parameters of the Hensel-Spittel model for AA6060.

A [MPa]	m_1 [1/°C]	m_2 [-]	m_3 [-]	m_4 [-]
509.203	-0.0063	0.032	0.1362	-0.00056

Simulation results. The simulation of the first set-up has been carried out with an initial temperature of 450°C for the tools and the workpiece. For the showed result, a punch speed of 1 mm/s has been used. The results have been evaluated at three different points P-1, P-2 and P-3 (Fig. 4 a), respectively at 1, 2 and 3 mm from the symmetry axis. These have been recorded from the moment a contact between the specimen and the stopper has been identified. From the results, it can be seen that the absolute value of stress triaxiality (Fig. 4 b), at the three evaluated points, remain low during the filling phase. On the other hand, as the filling process is completed and a full contact is reached, the hydrostatic pressure increases drastically, causing the recorded increase in stress triaxiality. The recorded Q-values show the integration of the criterion as soon as a contact at the evaluation point is found. It is possible to notice that the closer the evaluation point is to the symmetry axis, the longer the criterion will be integrated, reaching higher Q-values. According to the criterion, the welding quality decreases in radial direction.

The second set-up has been simulated at different temperatures and punch velocities in order to have a complete comparison of the three different welding criteria. The analyzed

temperatures have been 400, 450 and 550°C, while the punch speeds have been 1, 4 and 6 mm/s. All the criteria have been evaluated at the punch stroke of 2 mm.

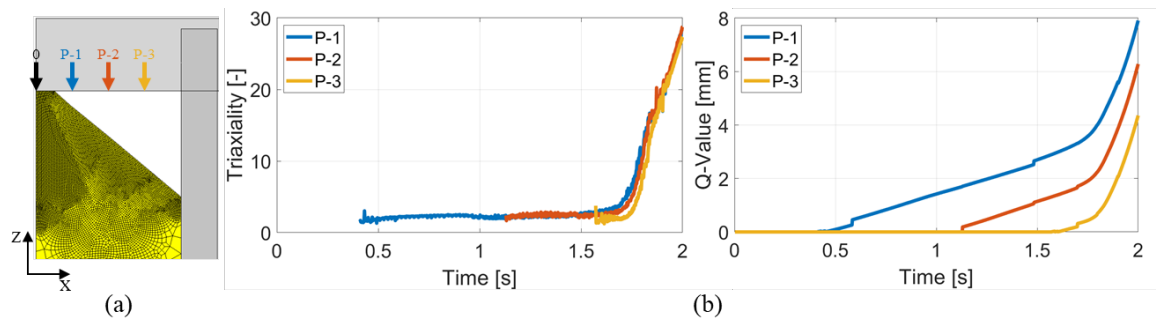


Fig. 4. (a) Position of evaluation points, (b) absolute value of triaxiality and Q-value over process time.

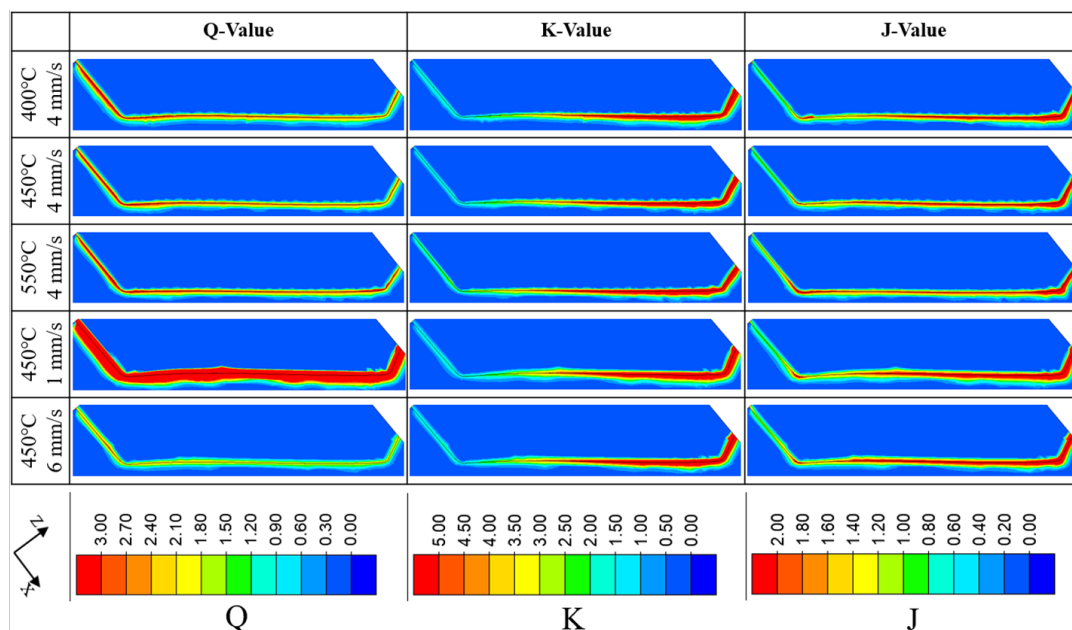


Fig. 5. Q-/K-/J-values at punch stroke 2 mm at different temperatures and punch speeds.

The results showed in Fig. 5 represent the contact interface between the specimens, as marked in Fig. 3 c. From the results, it is possible to see how the different criteria show different bonding conditions along the contact interface: the Q-value shows a relatively homogeneous welding status over the entire interface. Because of the formulation of the Q-criterion (integration of stress triaxiality over the time), the faster the punch speed is, the shorter the contact time is and therefore, the Q-criterion shows lower values for the simulation at 6 mm/s. On the other hand, the Q-criterion evaluated higher values at a slower punch speed (1 mm/s). The K value described an inhomogeneous welding condition over the interface: because of the smaller paths, covered by the material in the center of the probe, the criterion evaluates a lower welding condition in this region. Differently, higher values are calculated where the material velocity is higher, close to the punch edge. Since the contact time is not important during the evaluation of the K-value, all the simulations show similar results. Differently to the other criteria, the J-value considers also the effects of the temperature: because of the integration over the incremental strain, the results showed similarities to the K-value due to

the difference of strain rate along the contact interface, while it showed higher values as the temperature is increased.

FE Model of extrusion process

A methodology has been integrated within the FE-software PF-Extrude, in order to retrieve the welding zones and -further- evaluate quality criteria for the seam welds.

Extrusion tools. The industrial example showed in this study is manufactured by means of a two-hole extrusion tooling set-up (Fig. 6 a). Thanks to the symmetrical configuration, only half of the tools could have been used for further numerical analysis, in order to reduce the amount of elements and -therefore- save computational time. The CAD geometry has been processed in order to be implemented in the FE-simulation: the flow volume (which describes the material within the die) has been retrieved from the negative volume of the 3D geometries. This has been divided into different regions (Fig. 6 b): the portholes, which divide the material from the billet into different streams. The welding chamber, where the different streams are rejoined and weld together. The bearing, which helps to homogenize the exit velocities by changing the contact length of the tool with the material flow. The free surface, representing the extruded profile, is generated by prolonging the bearing lines. Moreover, on the bottom side of the die, the container is generated. The retrieved and generated surfaces have been discretized through a surface mesh, which is further used to generate the volumetric mesh representing the material during the FE-simulation.

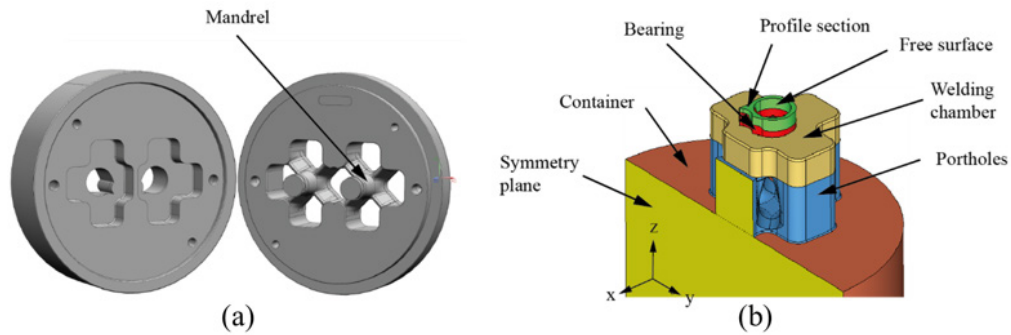


Fig. 6. (a) CAD model of extrusion tools, (b) retrieved flow volume for simulation.

Material modeling. The experimental data have been fitted through the Zener-Hollomon equation modified by Tong [9] (Eq. 5), in order to represent the yield behavior of the material during the extrusion simulations. The calculated fitting parameters are listed in table 2.

$$k_f(T, \dot{\varepsilon}, \varepsilon) = C \cdot \exp\left(\frac{Q}{R \cdot T}\right) \cdot \dot{\varepsilon}^m \cdot (1 - b \cdot \exp(-N \cdot \varepsilon)). \quad (5)$$

Table 2. Fitting parameters of the Zener-Hollomon-Tong for AA6060.

C [MPa]	Q [J/mol]	m [-]	b [-]	N [-]
0.2704	28078	0.1362	0.0992	4.7260

Friction modeling. Within the simulation of extrusion processes, it is critical to describe the frictional behavior of the material flowing in contact to the tools. For the purpose of this

analysis, the T-v-p friction model [10] by Becker has been used. Thereby, the shear frictional stress is computed as a function of pressure, relative velocity and temperature (Eq. 6 and 7). The experimental data, required for the model, have been retrieved by means of Tribo-Torsion tests [10], whereby the frictional behavior of the alloy (in contact with the tooling steel) is tested at different pressures, temperatures and relative velocities. The calculated fitting parameters can be found in table 3.

$$\tau(T, v, p) = \left\{ \tau_{\max} - (\tau_{\max} - \tau_{\min}) \exp \left[-q \left(\frac{p}{p_0} \right)^n \right] \right\} \left(\frac{v}{v_0} \right)^k \left(\frac{T}{T_0} \right)^m \quad (6)$$

whereby:

$$\tau_{\max} = \frac{k_f(T, \dot{\varepsilon} = 1000, \varepsilon = 0.2)}{\sqrt{3}}, \tau_{\min} = 0.2 \cdot \tau_{\max} \quad (7)$$

Table 3. Fitting parameters of the T-v-p friction model.

q [-]	n [-]	k [-]	m [-]	p ₀ [MPa]	v ₀ [mm/s]	T ₀ [°C]
9.683	1.205	0.005	0.875	100	50	660

Seam welds analysis strategy

Description of algorithm. In the literature, it is possible to find various studies that rely on particles tracking algorithms to -accurately- analyze the position of the seam welds as shown in the research by Kloppenborg et al. [11]. A particle-tracking algorithm has been implemented in the FE-code PF-Extrude in order to analyze the charge weld evolution during the billet-to-billet extrusion process [12]. This algorithm has been further developed in order to suit the requirements for a quality analysis of the seam welds. The routine has been implemented within the extrusion simulation, such that it is called at the end of every time increment as the material flow is updated. The first time the routine is called, a search of the portholes is executed and the different channels are recognized by analyzing the connectivity of the elements within the volumetric mesh (Fig. 7 a). Being the material in proximity of the tools responsible for the bonding of the different material streams, only the boundary elements of the mesh are considered. As these are retrieved at an arbitrary section of the die, particles are positioned within these and assigned an identification code specific to the porthole they reside (Fig. 7 b). Further, the particles are allowed to flow within the discretized volume, following the previously simulated velocity field.

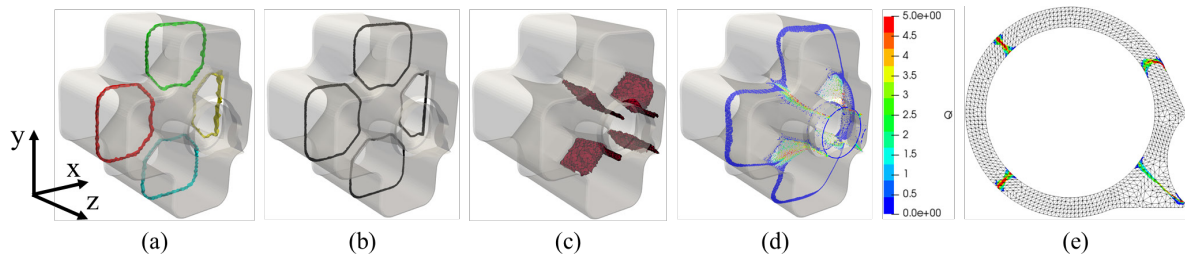


Fig. 7. Description of seam welds analysis algorithm: (a) identification of portholes, (b) particles positioning, (c) retrieval of welding zones, (d) tracking for quality criterion integration, (e) seam welds positions and quality.

As particles with different identification codes reach the same elements, these are marked as welding zones (Fig. 7 c). Once the particle tracking terminates, the particles are transferred back at their starting positions and tracked a second time. Within this final step of the analysis, quality criteria are evaluated as the particles cross elements previously identified as welding zones (Fig. 7 d). The results can be evaluated at the profile section of the simulation, where the position and the quality of the seam welds can be visualized (Fig. 7 e). In the showed industrial example, ca. 18'900 particles have been tracked during the seam welds analysis and the execution time of the whole routine (after the first simulation increment) required 240 s on six Intel Xeon CPU E5-2697 v3 cores with 64 GB RAM.

Particle-tracking algorithm. As the boundary elements within the region of the portholes are isolated, the routine generates particles on the section crossing these. Only particles that lie within the isolated elements are selected for the tracking algorithm. In order to retrieve the position of the particles within the enclosing element, the barycentric coordinates of each particle, relatively to this, are calculated. Further, the velocity vector is interpolated from the nodes of the enclosing element. A more detailed description of the algorithm can be found in [12]. The particle tracking is continued until a user given percentage of particles reach the profile section during the simulation: since some particles could land in dead metal zones and -therefore- not contribute to the evaluation of the seam welds, a limit to particles, that must reach the profile section, is defined. By default, this value is set to 90%, which delivered stable results during the execution of the routine.

Conclusions

A seam weld quality algorithm integrated in the FE-code PF-Extrude has been presented, whereby, by means of a particle-tracking algorithm, the welding zones within the die can be isolated and the different welding criteria (Q, K, J) can be evaluated at the profile section of the extrudate. In order to calibrate the welding criteria, two different experiments are proposed, whereby the different criteria has been analyzed through FE-simulations with the commercial software simufact.forming. The results highlighted the differences between the criteria, showing dissimilar welding conditions along the contact interface of the specimens. In outlook, the simulations shall be validated through physical experiments and the contact interface between the specimens investigated through microstructure analysis. Furthermore, the results from the experiments shall be compared with the results from this study, in order to evaluate the welding conditions and limits of the considered aluminium alloy.

Acknowledgements

The authors would like to express their gratitude to the Commission for Technology and Innovation, and to the company Aluminium Laufen AG for the support. The study is part of the CTI-project 19306.1 PFIW-IW.

References

- [1] M. Plata, J. Piwnik: *Theoretical and experimental analysis of seam weld formation in hot extrusion of aluminum alloys*, Proceedings of Seventh International Aluminium Extrusion Technology Seminar ET, vol. 1 (2000), pp. 205-211.

- [2] L. Donati, L. Tomesani: *The prediction of seam welds quality in aluminum extrusion*, Journal of Materials Processing Technology, vol. 153-154 (2004), pp. 366-373.
- [3] H. Valberg: *Extrusion welding in aluminium extrusion*, International Journal of Materials and Product Technology, vol. 17 (7) (2002), pp. 497-556.
- [4] H. Valberg, T. Loeken, M. Hval, B. Nyhus, C. Thaulow: *The extrusion of hollow profiles with a gas pocket behind the bridge*, International Journal of Materials and Product Technology, vol. 10 (3-6) (1995), pp. 222-267.
- [5] J. Yu, G. Zhao, L. Chen: *Analysis of longitudinal weld seam defects and investigation of solid-state bonding criteria in porthole die extrusion process of aluminum alloy profiles*, Journal of Materials Processing Technology, vol. 237 (2016), pp. 31-47.
- [6] E. Ceretti, L. Fratini, F. Gagliardi, C. Giardini: *A new approach to study material bonding in extrusion porthole dies*, CIRP Annals – Manufacturing Technology, vol. 58 (1) (2009), pp. 259-262.
- [7] S. W. Bai, G. Fang, J. Zhou, *Analysis of the bonding strength and microstructure of AA6082 extrusion weld seams formed during physical simulation*, Journal of Materials Processing Tech., vol. 250 (2017), pp. 109-120.
- [8] L. Tong, C. Becker, P. Hora: *High efficiency in the simulation of complex extrusion processes using an advanced simulation method*, Materials Today: Proceedings, vol. 2 (10) (2015), pp. 4726 – 4731.
- [9] L. Tong, S. Stahel, P. Hora: *Modeling for the FE-simulation of warm metal forming processes*, Numisheet, vol. 778 (1) (2005), pp. 625-629.
- [10] C. Becker, P. Hora, J. Maier, S. Müller: *Experimental investigations of friction carried out with the Tribo-Torsion-Test and friction modelling*, Key Engineering Materials, vol. 585 (2013), pp. 25-32.
- [11] T. Kloppenborg, N. Ben Khalifa, A. E. Tekkaya: *Accurate welding line prediction in extrusion processes*, Key Engineering Materials, vol. 424 (2009), pp. 87-95.
- [12] M. Crosio, D. Hora, C. Becker, P. Hora: *Realistic representation and investigation of charge weld evolution during direct porthole die extrusion processes through FE-analysis*, Procedia Manufacturing, vol. 15 (2018), pp. 232-239.